



# Numerical analysis of adiabatic flow of refrigerant through a spiral capillary tube

M.K. Mittal, Ravi Kumar\*, Akhilesh Gupta

Department of Mechanical and Industrial Engineering, Indian Institute of Technology, Roorkee 247667, India

## ARTICLE INFO

### Article history:

Received 17 September 2008

Received in revised form 24 December 2008

Accepted 5 January 2009

Available online 17 March 2009

### Keywords:

Spiral tube

Capillary tube

Pitch

Metastable flow

Two phase flow

Homogenous flow

## ABSTRACT

In the present work, a homogenous model including the metastable liquid region has been developed for the adiabatic flow of refrigerant through the spiral capillary tube. In order to develop the model, both liquid region and two phase region have been discretized into infinitesimal segments to take into account the effect of varying radius of curvature of spiral tube on the friction factor. The effect of the pitch of spiral on the mass flow rate of refrigerant and capillary tube length has been investigated. A comparison of flow characteristics of refrigerant R22 and its alternatives, i.e., R407C and R410A has been made at different operating conditions at the inlet of the capillary tube and it has been found that the flow characteristics of R22 and R407C are almost similar for a given condenser pressure and degree of subcooling at the inlet of capillary tube.

© 2009 Elsevier Masson SAS. All rights reserved.

## 1. Introduction

Capillary tubes are widely used as an expansion and metering device in small capacity refrigeration systems and air-conditioners where the cooling load is fairly constant. In spite of simple configuration, the flow behaviour of refrigerant through capillary tube is a complex phenomenon. A number of experimental and numerical studies have been conducted in the past to understand the flow characteristics of refrigerant through a capillary tube, as the behaviour of capillary tube is crucial to the performance of the refrigeration system. Due to concern of ozone layer depletion and global warming, the use of conventional refrigerants has been prohibited; hence the redesign and analysis of flow through capillary tubes with new alternative refrigerants has received the considerable attention in the recent years.

A capillary tube can have the geometries of straight, helical and spiral shape. Kuehl and Goldschmidt [1] pioneered the experimental study on the coiled tube to determine the effect of coiling on the mass flow rate of refrigerant through the coiled capillary tube and they observed that the mass flow rate of refrigerant through a coiled tube is approximately 0–5 percent lower than that through a straight tube. Wei et al. [2] compared the performance of straight and coiled capillary tubes for the flow of R22 and R407C and concluded that the mass flow rate through the coiled tube is about 10–15 percent lower than that through the straight tube. Wei et al. [3] examined the performance difference between the straight and coiled capillary tubes working with R22 and observed that the

effect of helical shape increases as the coil diameter decreases. Kim et al. [4] developed a dimensionless correlation to predict mass flow rates through adiabatic coiled capillary tubes for the flow of refrigerant R22, R407C and R410A. Zhou and Zhang [5] carried out an experimental study on coiled tube with refrigerant R22 and found that the coiling effect is insignificant beyond a coil diameter of 300 mm. Park et al. [6] examined the performance of coiled capillary tubes having R22 as the working fluid and reported that mass flow rates through the coiled capillary tubes decreased by 5–16 percent than those through the straight capillary tubes. Khan et al. [7] investigated the effect of coil pitch of helical capillary tube on the mass flow rate and reported that the mass flow rate through coiled tubes having pitch 20, 40 and 60 mm is reduced by 17, 12 and 8.5 percent respectively in comparison to the mass flow rate through straight capillary tube. Khan et al. [8] also conducted parametric study for straight and spirally coiled capillary tubes with R134a as the working fluid and observed that the coiling results in reduction of mass flow rate by 5–15 percent in comparison to the mass flow rate through straight tube.

Gorasia et al. [9] developed a mathematical model for the coiled capillary tubes. They used Mori and Nakayama [10] equation and Giri correlation (cited from [9]) to determine single phase and two phase flow friction factor. A comparative study of different combinations of friction factor and viscosity correlations for prediction of refrigerant flow through capillary tubes has been made by Zhang et al. [11]. A numerical model for adiabatic coiled capillary tubes considering separated flow model and metastable regions has been developed by Garcia-Valladares [12]. Khan et al. [13] also formulated a homogenous flow model for adiabatic helical capillary tubes by incorporating pitch of helix as a parameter

\* Corresponding author. Tel.: +91 1332 285740; fax: +91 1332 285665.

E-mail address: ravikfme@iitr.ernet.in (R. Kumar).

**Nomenclature**

$A$	cross sectional area of capillary tube	$\text{m}^2$
$d_c$	capillary tube diameter	$\text{m}$
$D$	coil diameter	$\text{m}$
$D'$	reference length	$\text{m}$
$De$	Dean number $Re(d/D)^{0.5}$	
$e$	roughness height	$\text{m}$
$f$	friction factor	
$G$	mass velocity	$\text{kg m}^{-2} \text{s}^{-1}$
$h$	specific enthalpy	$\text{J kg}^{-1}$
$K$	entrance loss coefficient	
$k_B$	Boltzmann constant	$1.38066 \times 10^{-23} \text{ J K}^{-1}$
$L$	capillary tube length	$\text{m}$
$\dot{m}$	mass flow rate	$\text{kg s}^{-1}$
$P$	pressure	$\text{Pa}$
$p$	pitch	$\text{m}$
$R$	radius of curvature of coil	$\text{m}$
$Re$	Reynolds number	
$t$	temperature	$^{\circ}\text{C}$
$T_c$	critical temperature	$^{\circ}\text{C}$
$V$	fluid velocity	$\text{m s}^{-1}$
$v$	specific volume	$\text{m}^3 \text{kg}^{-1}$
$x$	quality	

**Greek letters**

$\mu$	viscosity	$\text{Pa s}$
$\rho$	density	$\text{kg m}^{-3}$
$\sigma$	surface tension	$\text{N m}^{-1}$
$\theta$	angle	radian
$\tau_w$	wall shear stress	$\text{N m}^{-2}$
$\Delta T_{\text{sub}}$	degree of subcooling	$^{\circ}\text{C}$

**Subscripts**

$c$	coil, capillary
$f$	saturated liquid
$g$	saturated vapour
$fg$	liquid–vapour mixture
$i$	ith element, inlet
$k$	condenser
$m$	mean
$meta$	metastable
$o$	outlet
$s$	straight, saturated
$sp$	single phase
$sub$	subcooling
$tp$	two phase

in their mathematical model. A mathematical model for spiral capillary tube was also developed by them [14].

Capillary tubes are usually coiled, normally in helical shape, to save the space. A number of studies, theoretical and experimental, had been performed on helical capillary tube. Another way of coiling the capillary is to coil into spiral shape. Relatively little information in open literature is available on flow characteristics of refrigerants in spiral capillary tube. The objective of present study is to develop a numerical model to understand the basic physics of refrigerant flow in spiral capillary tube.

A mathematical model based on two phase homogenous flow has been proposed to study the performance of adiabatic spiral capillary tubes. REFPROP 7.0 database [15] based on the Carnahan–Starling–Desantis equation of state has been used to determine the thermodynamic and transport properties of the refrigerant.

## 2. Mathematical modelling

A mathematical model has been developed by dividing the flow of refrigerant through capillary tube in three distinct regimes, viz., single phase subcooled liquid regime, metastable liquid regime and two phase liquid vapour regime. The flow through two phase liquid vapour regime has been considered homogenous flow, i.e., the liquid and vapour phases have the same velocity. The basic governing equations used to describe the flow characteristics are developed from conservation equation of mass, momentum and energy.

In Fig. 1, there is a pressure drop between point 1 and 2 due to sudden contraction at the inlet of capillary tube. The refrigerant is subcooled liquid in the region 2–3 followed by a metastable region 3–4, where the refrigerant remains in thermodynamic non-equilibrium state. The two phase region lies between points 4 and 5, where the pressure drop varies rapidly along the length of the tube due to phase change of liquid refrigerant to vapour. The numerical model has been developed on the assumptions that the spiral capillary tube is of uniform cross section and surface roughness, the flow through the capillary tube is homogenous, adiabatic, one-dimensional and fully developed turbulent flow.

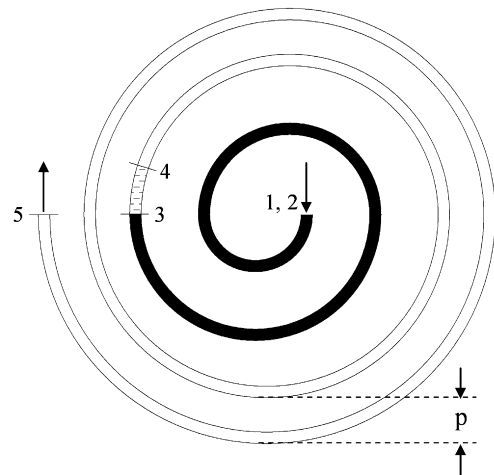


Fig. 1. Computational domain of spiral capillary tube.

A free body diagram of elemental length,  $dL$ , is shown in Fig. 2a. Applying momentum conservation along  $x$ -direction on the fluid element of length,  $dL$ :

$$P A \cos(d\theta/2) - (P + dP) A \cos(d\theta/2) - 2\tau_w \pi d_c (dL/2) \cos(d\theta/4) = \dot{m} dV \cos(d\theta/2) \quad (1)$$

Since  $\dot{m} = GA$  and  $\tau_w = f\rho V^2/8$ , on simplification Eq. (1) reduces to the following equation (2)

$$dL = \frac{2d_c}{f} \left( \frac{-\rho dP}{G^2} + \frac{d\rho}{\rho} \right) \frac{\cos(d\theta/2)}{\cos(d\theta/4)} \quad (2)$$

The pressure drop due to entrance effect can be determined by the following equation (3)

$$P_1 - P_2 = K \frac{\rho V^2}{2} \quad (3)$$

where, 'K' is the entrance loss coefficient. The value of 'K' is taken as 1.5 from Zhou and Zhang [5].

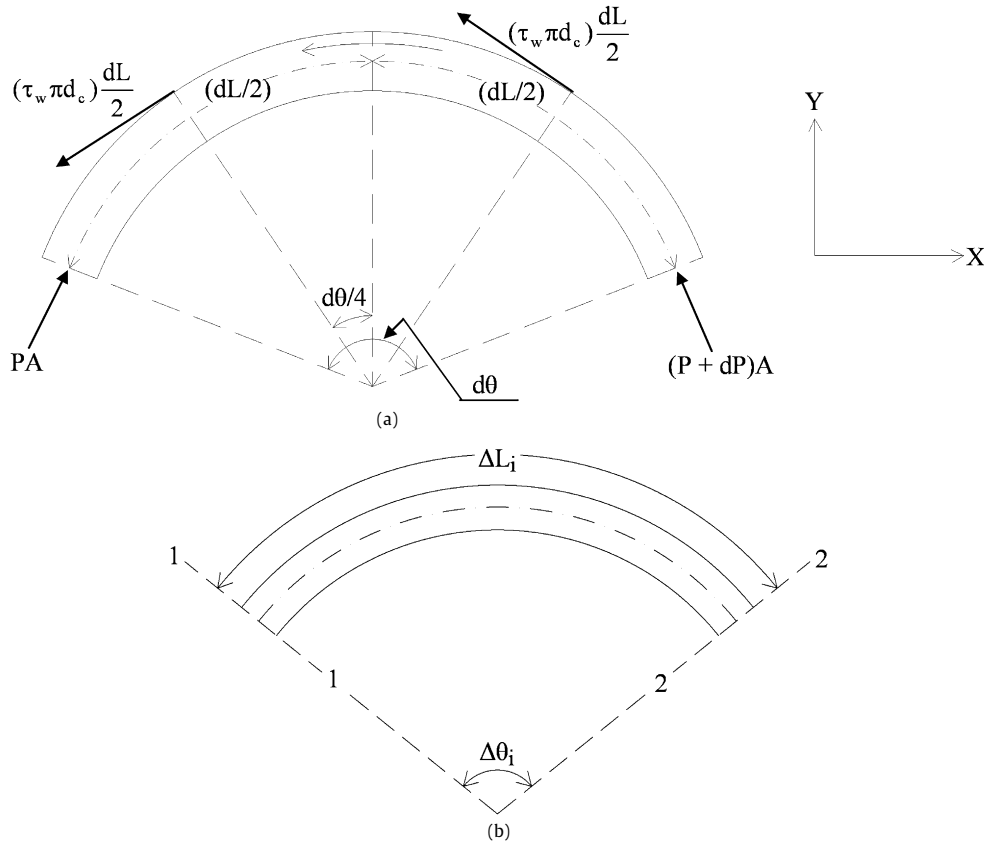


Fig. 2. (a) Free body diagram of fluid element; (b) Schematic diagram of  $i$ th element.

The subcooled single phase liquid is considered as incompressible, hence Eq. (2) for single phase flow through spiral capillary tube can be written as:

$$dL = \frac{2d_c}{f_{csp}} \left( \frac{-\rho dP}{G^2} \right) \frac{\cos(d\theta/2)}{\cos(d\theta/4)} \quad (4)$$

The single phase friction factor for coiled tube,  $f_{csp}$ , is calculated from the Ju et al. [16] correlation as follows:

For turbulent flow, with  $De > 11.6$

$$f_{csp} = f_s (1 + 0.11 Re^{0.23} (d_c/D)^{0.14}) \quad (5)$$

$$\text{where, } f_s = 0.1 (1.46e/d_c + 100/Re)^{0.25} \quad (6)$$

The coil diameter,  $D$  in the above friction factor correlation may suitably be replaced by twice the radius of curvature, i.e.,  $D = 2R$ . A spiral coil is a coil of varying radius of curvature. The radius of curvature for the Archimedes spiral having pitch,  $p$ , is given by the following equation:

$$R(\theta) = \frac{(p/2\pi)(1 + \theta^2)^{1.5}}{2 + \theta^2} \quad (7)$$

and the length of Archimedes spiral is given by:

$$L(\theta) = \frac{p}{4\pi} [\theta \sqrt{1 + \theta^2} + \ln(\theta + \sqrt{1 + \theta^2})] \quad (8)$$

Differentiating Eq. (8) with respect to  $\theta$  and after rearranging, the following equation (9) is obtained.

$$d\theta = \frac{2\pi dL}{p\sqrt{1 + \theta^2}} \quad (9)$$

To determine the single phase length, single phase region is divided into 'n' number of small elements having equal pressure differential,  $\Delta P$ , to take into account the effect of varying radius

of curvature on the friction factor. The pressure differential,  $\Delta P$ , is given by:

$$\Delta P = (P_2 - P_3)/n \quad (10)$$

where,  $P_3$  is the saturation pressure corresponding to the temperature of refrigerant at the inlet of capillary tube.

The discretized form of Eqs. (4) and (9) for  $i$ th element can be written as:

$$\Delta L_i = \frac{2d_c}{f_{cspi}} \left( \frac{-\rho \Delta P}{G^2} \right) \frac{\cos(\Delta\theta_i/2)}{\cos(\Delta\theta_i/4)} \quad (11)$$

$$\Delta\theta_i = \frac{2\pi \Delta L_i}{p\sqrt{1 + \theta_i^2}} \quad (12)$$

Schematic diagram of  $i$ th element has been shown in Fig. 2b. To calculate  $\Delta L_i$ , first of all  $\Delta\theta_i$  is assumed to determine  $\theta_i$  for the  $i$ th element. The angle  $\theta_i$  for the  $i$ th element is calculated as follows:

$$\theta_i = \theta_{i-1} + \Delta\theta_i/2 \quad (13)$$

where,  $\theta_{i-1}$  is the angle at the inlet of  $i$ th element.

The angle,  $\theta_i$  is used to evaluate the radius of curvature of capillary tube using Eq. (7) and the friction factor for the  $i$ th element is determined from Eq. (5). The elemental length,  $\Delta L_i$ , determined from Eq. (11) is substituted in Eq. (12) to calculate new value of  $\Delta\theta_i$ . These calculation steps are repeated till the convergence of  $\Delta\theta_i$  for the  $i$ th element is attained. Finally all the  $\Delta L_i$  are added to determine the single phase length.

In order to evaluate metastable liquid length, Chen et al. [17] correlation represented by Eq. (14) has been used to determine the pressure difference between the theoretical flashing point and actual flashing point, i.e.,  $P_s - P_v$  or  $P_3 - P_4$ .

$$\frac{(P_s - P_v)\sqrt{k_B T_s}}{\sigma^{1.5}} = 0.679 \left( \frac{v_g}{v_{fg}} \right) Re^{0.914} \left( \frac{\Delta T_{sub}}{T_c} \right)^{-0.208} \left( \frac{d_c}{D'} \right)^{-3.18} \quad (14)$$

where  $D'$  is the reference length given by  $D' = 10000 \sqrt{\frac{k_B T_s}{\sigma}}$ .

The metastable liquid length is determined as:

$$L_{meta} = \frac{2d_c}{f_{cspmeta}} \left( \frac{-\rho(P_3 - P_4)}{G^2} \right) \frac{\cos(\Delta\theta_{meta}/2)}{\cos(\Delta\theta_{meta}/4)} \quad (15)$$

where,  $f_{cspmeta}$  is a friction factor for metastable flow, which is calculated from the same friction factor equation as that for single phase flow represented by Eq. (5) and  $\Delta\theta_{meta}$  is the angle subtended by the metastable liquid length.

The flow of refrigerant in two phase flow region has been modelled as homogenous flow. The two phase flow region is divided into small elements with uniform pressure drop across each element.

Applying conservation of energy equation between inlet and outlet of an element lying in the two phase region:

$$h_i + \frac{V_i^2}{2} = h_{fo} + x_o h_{fgo} + \frac{G^2}{2} (v_{fo} + x_o v_{fgo})^2 \quad (16)$$

In the above equation the parameters at the inlet of element are known and since the pressure at the outlet of the element is also known, thus the saturated liquid and vapour properties corresponding to the known pressure at the outlet of element can be determined from REFPROP 7.0 database [15]. Thus the only unknown in Eq. (16) is quality,  $x_o$ , which is evaluated analytically. Then the thermodynamic and transport properties of the refrigerant at the outlet of the element can be determined from the known value of quality,  $x_o$ , and pressure,  $P_o$ .

Finally the elemental length,  $\Delta L$ , is calculated by using discretized form of Eq. (2) for the two phase flow as given below:

$$\Delta L = \frac{2d_c}{f_{ctpm}} \left( \frac{-\rho_m \Delta P}{G^2} + \frac{\Delta \rho}{\rho_m} \right) \frac{\cos(\Delta\theta/2)}{\cos(\Delta\theta/4)} \quad (17)$$

where,  $\rho_m$  and  $f_{ctpm}$  are mean density and mean friction factor respectively over the control volume in the two phase region and the method followed to evaluate the elemental length is same as discussed in calculating the elemental length in single phase flow.

The two phase friction factor for coiled tube,  $f_{ctp}$  is determined from Eq. (5) with the Reynolds number for two phase flow defined by the following equation (18).

$$Re_{tp} = \frac{G d_c}{\mu_{tp}} \quad (18)$$

The two phase viscosity,  $\mu_{tp}$ , is calculated from Dukler's correlation [18], as it has been suggested by Wong et al. [19] that Dukler mixture viscosity expression [18] gives the best prediction when used for the homogenous model.

$$\mu_{tp} = \frac{x v_g \mu_g + (1-x) v_f \mu_f}{x v_g + (1-x) v_f} \quad (19)$$

Thus, the elemental lengths,  $\Delta L$ , in the two phase region are determined step-by-step from point 4, shown in Fig. 1, to the exit of the capillary tube. The entropy is also calculated simultaneously at the outlet of each element and it has been found that the entropy gradually increases along the direction of flow and after reaching a certain value; it starts decreasing, which is the violation of the second law of thermodynamics. This point of negative entropy change is used as a criterion to detect the choked flow condition in the capillary tube and the calculation is terminated at this point of maximum entropy. The pressure at the outlet of the element is also compared with the evaporator pressure and if

**Table 1**

Parameters used for validation of numerical results with the experimental results of Khan et al. [8].

Parameters	Value
Refrigerant	R-134a
Capillary tube length ( $L$ ), m	2.4, 3.2, 4.0, 4.8, 5.6, 6.4
Capillary tube diameter ( $d_c$ ), mm	1.12, 1.4, 1.63
Relative roughness of capillary tube ( $e/d_c$ )	0.0063, 0.0044, 0.0022
Pitch of spiral coil ( $p$ ), mm	20, 40, 60
Condenser pressure ( $P_k$ ), kPa	740
Degree of subcooling ( $\Delta T_{sub}$ ), °C	0–20
Uncertainty in the measurement of mass flow rate	0.5 kg/h
Uncertainty in the measurement of pressure drop	2.6 kPa
Position of spiral capillary tube	Horizontal

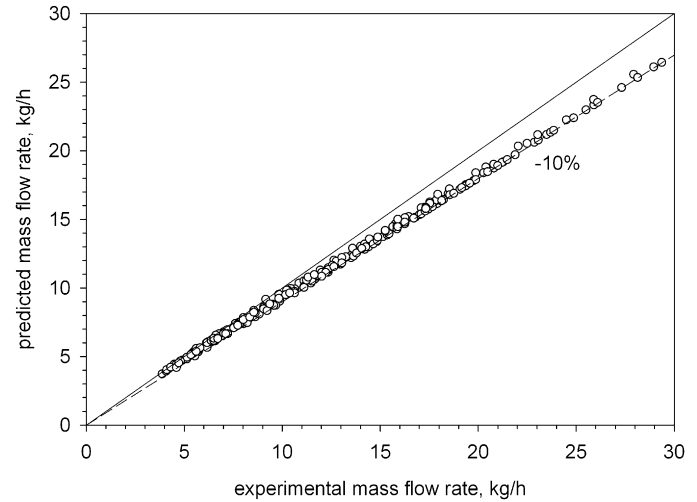


**Fig. 3.** Comparison of proposed model with experimental data of Khan et al. [8].

the outlet pressure becomes equal to the evaporator pressure before reaching the choked condition, the calculation is terminated at this point and flow in this condition is said to be unchoked. Finally, all the elemental lengths,  $\Delta L$ , are added to calculate the two phase length,  $L_{tp}$ .

### 3. Results and discussion

In order to validate the present model, comparisons of the numerical results have been made with the experimental results of Khan et al. [8] which is the only experimental study available in the literature for adiabatic spiral capillary tube.

Khan et al. [8] presented their experimental results in terms of mass flow rate of refrigerant R-134a for different capillary tube length, capillary tube diameter, pitch of spiral and degree of subcooling. The geometrical parameters and operating conditions used by Khan et al. [8] are shown in Table 1. The pressure at capillary inlet for all experimental runs was maintained constant at 740 kPa. For a particular test section, four to five level subcoolings were taken in the range of 0–20 °C. The pressure at the exit of capillary was kept below the critical pressure. Hence all the numerical cases evaluated for the validation of the model present choke exit conditions.

Fig. 3 shows the comparison of experimental mass flow rate of Khan et al. [8] and numerical mass flow rate predicted by the proposed model. It may be observed that the numerical mass flow rates calculated for all the 239 data sets underpredict the experimental mass flow rates within a range of zero to –10 percent and the mean deviation is –7.9 percent.

In this section, the output from the model has been used to investigate the effect of pitch of spiral on the mass flow rate of the

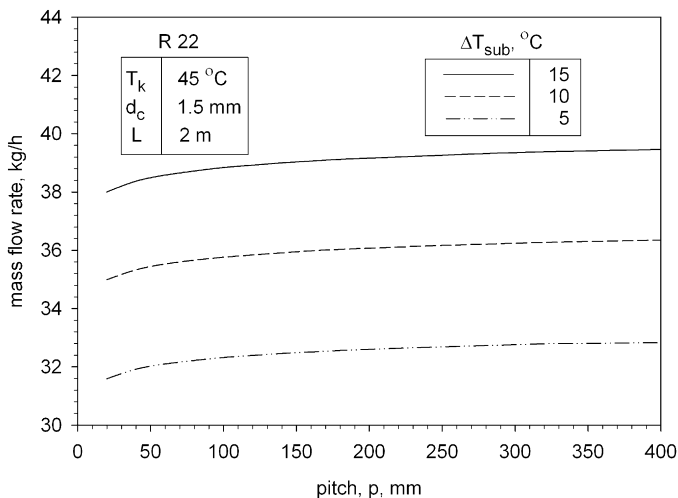


Fig. 4. Effect of coil pitch on mass flow rate.

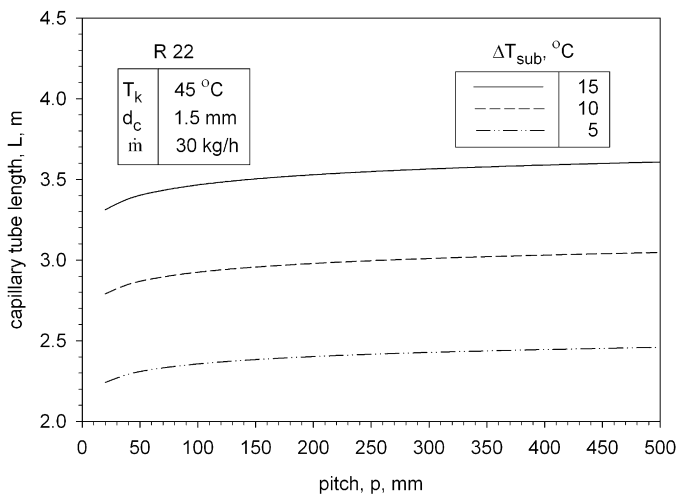


Fig. 5. Effect of coil pitch on capillary tube length.

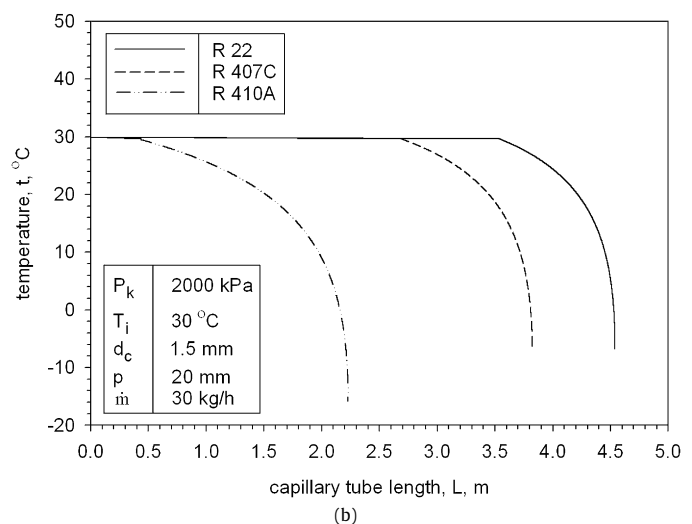
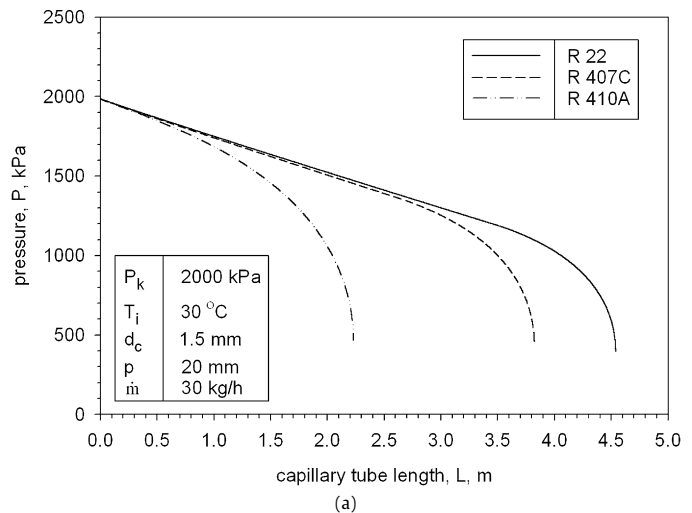


Fig. 6. Pressure and temperature distribution at same condenser pressure and same inlet temperature for refrigerant R22, R407C and R410A.

refrigerant and the length of the capillary tube. Moreover, comparison of flow characteristics of R22 and its alternatives, i.e., R407C and R410A has been made under different conditions at the inlet of capillary tube.

Fig. 4 has been drawn to show the effect of spiral pitch on the mass flow of refrigerant. It is quite apparent that the mass flow rate of refrigerant increases with the rise in spiral pitch. The increase in spiral pitch reduces the coil curvature which results in reduction of friction factor, thus the mass flow of refrigerant flowing through a capillary tube increases. The mass flow rate of refrigerant is increased by about 2.46 percent as the coil pitch increases from 20 to 120 mm. The rising trend of mass flow rate decreases as the pitch increases and beyond a pitch of 120 mm, the increase in mass flow rate is quite sluggish.

The effect of spiral pitch on the capillary tube length has been shown in Fig. 5. It is observed that capillary tube length increases as the spiral pitch increases. This is due to the fact that the friction factor decreases as the coil pitch increases because of reduction in coil curvature with the increase in coil pitch. Hence, for the same mass flow rate, the pressure drop distribution along the capillary tube length decreases as the pitch increases resulting in increased choking length of the capillary tube. With the coil pitch increasing from 20 to 120 mm, the capillary tube length increases by 5.37 percent. The increase in capillary tube length is very little, when the pitch is increased beyond a value of 120 mm.

Fig. 6 describe the pressure and temperature distribution along the capillary tube for refrigerant R22, R407C and R410A at the same condenser pressure and same temperature at the inlet of capillary tube. The total pressure drop across the capillary tube is almost same for all these refrigerants, but there is a large difference in the capillary tube length. At a condenser pressure of 2000 kPa and inlet temperature of 30 °C, the inlet degree of subcooling for R22, R407C and R410A are 21.27, 15.59 and 2.22 °C respectively. Since the degree of subcooling for refrigerant R22 is the highest, therefore it can be clearly noticed from Fig. 6b that the single phase length and hence the total capillary tube length is the longest for refrigerant R22.

Fig. 7 presents the pressure and temperature distribution along the capillary tube for refrigerant R22, R407C and R410A at the same condenser temperature and same degree of subcooling at the inlet of capillary tube. At the same condenser temperature, the saturation pressure of R410A and R407C is higher than that of R22. Higher pressure at the capillary tube inlet results in higher capillary tube length for the same mass flow rate. That is why the capillary tube length is higher for refrigerant R410A and R407C than that for refrigerant R22 at the same condenser temperature and mass flow rate. The difference in temperature distribution is also large due to large difference in pressure distribution.

Fig. 8 has been drawn to depict the pressure and temperature distribution along the capillary tube for refrigerant R22, R407C and

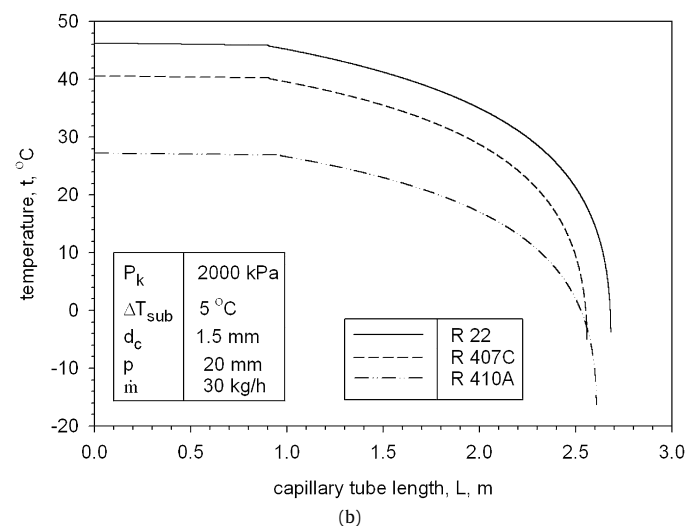
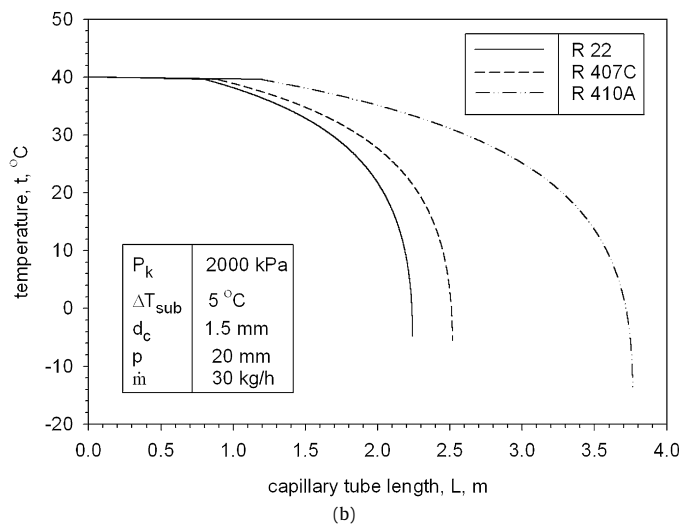
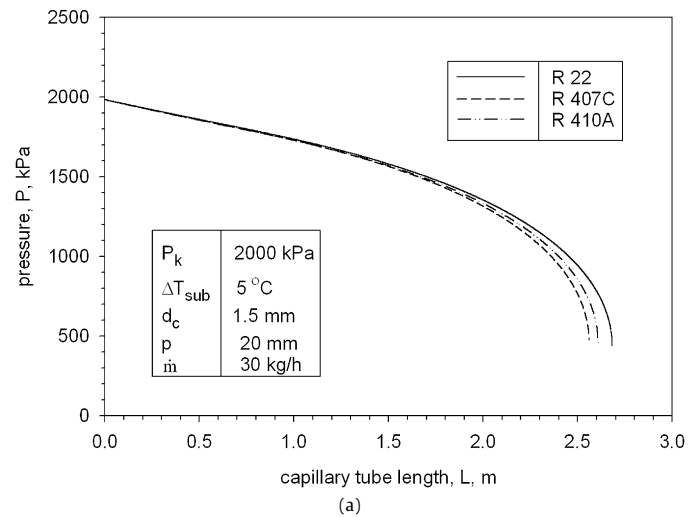
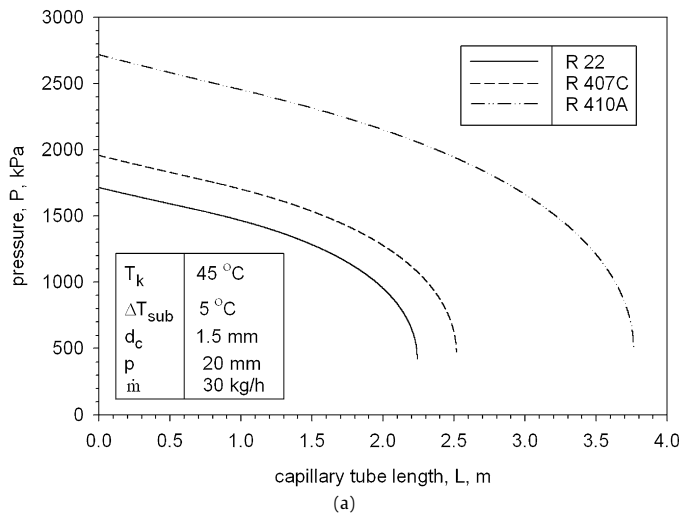


**Fig. 7.** Pressure and temperature distribution at same condenser temperature and same degree of subcooling for refrigerant R22, R407C and R410A.

**Fig. 8.** Pressure and temperature distribution at same condenser pressure and same degree of subcooling for refrigerant R22, R407C and R410A.

R410A at the same condenser pressure and same degree of subcooling at the inlet of capillary tube. Fig. 8a shows that there is little difference in pressure distribution for these refrigerants. Since the capillary tube length depends on the operating conditions at the inlet of capillary tube and pressure distribution along the capillary tube, therefore capillary tube length for these refrigerants is also almost same. Fig. 8b shows that the exit temperature for refrigerant R22 and R407C is also almost same, however the exit temperature of R410A is much lower. So, it can be said that the flow characteristics of R22 and R407C are almost same at the same condenser pressure and same degree of subcooling at the inlet of capillary tube.

#### 4. Conclusions

The model developed has been validated with the available experimental results and presents reasonably well in the range of 0 to –10 percent. The results obtained from the model by varying the input operating and geometrical parameters of the capillary tube lead to the following conclusions:

1. The mass flow rate increases with increase of pitch. However, for a capillary tube of 1.5 mm diameter and 2 m length, the rise in mass flow rate is quite slow beyond a pitch of 120 mm.

2. On increasing the coil pitch, capillary tube length increases and the rising trend becomes monotonous beyond a pitch of 120 mm for a capillary tube of 1.5 mm diameter and 2 m length.
3. The flow characteristics of R22 and R407C are quite similar at the same condenser pressure and same degree of subcooling.

#### References

- [1] S.J. Kuehl, V.W. Goldschmidt, Steady flows of R-22 through capillary tubes: Test data, *ASHRAE Trans.* 96 (1) (1990) 719–728.
- [2] C.Z. Wei, Y.T. Lin, C.C. Wang, J.S. Leu, An experimental study of the performance of capillary tubes for R-407C refrigerant, *ASHRAE Trans.* 105 (2) (1999) 634–638.
- [3] C.Z. Wei, Y.T. Lin, C.C. Wang, A performance comparison between coiled and straight capillary tubes, *Heat Transfer Eng.* 21 (2) (2000) 62–66.
- [4] S.G. Kim, M.S. Kim, S.T. Ro, Experimental investigation of the performance of R-22, R-407C and R-410A in several capillary tubes for air conditioners, *Int. J. Refrigeration* 25 (5) (2002) 521–531.
- [5] G. Zhou, Y. Zhang, Numerical and experimental investigations on the performance of coiled adiabatic capillary tube, *Appl. Thermal Eng.* 26 (11–12) (2006) 1106–1114.
- [6] C. Park, S. Lee, H. Kang, Y. Kim, Experimentation and modeling of refrigerant flow through coiled capillary tube, *Int. J. Refrigeration* 30 (7) (2007) 1168–1175.
- [7] M.K. Khan, R. Kumar, P.K. Sahoo, Experimental study of the flow of R-134a through an adiabatic helically coiled capillary tube, *HVAC&R Research* ASHRAE 14 (5) (2008).

- [8] M.K. Khan, R. Kumar, P.K. Sahoo, An experimental study of the flow of R-134a inside an adiabatic spirally coiled capillary tube, *Int. J. of Refrigeration* 31 (2008) 969–977.
- [9] J.N. Gorasia, N. Dubey, K.K. Jain, Computer-aided design of capillaries of different configurations, *ASHRAE Trans.* 97 (1) (1991) 132–138.
- [10] Y. Mori, W. Nakayama, Study on forced convective heat transfer in curved pipes (2nd, report turbulent region), *Int. J. Heat Mass Transfer* 10 (1967) 37–59.
- [11] Y. Zhang, G. Zhou, X. Hui, C. Jing, An assessment of friction factor and viscosity correlations for model prediction of refrigerant flow in capillary tubes, *Int. J. Energy Res.* 29 (2005) 233–248.
- [12] O. Garcia-Valladares, Numerical simulation and experimental validation of coiled adiabatic capillary tubes, *Appl. Thermal Eng.* 27 (2007) 1062–1071.
- [13] M.K. Khan, R. Kumar, P.K. Sahoo, A homogeneous flow model for adiabatic helical capillary tube, *ASHRAE Trans.* 114 (1) (2008) 239–247.
- [14] M.K. Khan, R. Kumar, P.K. Sahoo, Flow characteristics of refrigerants flowing inside an adiabatic spiral capillary tube, *HVAC&R Research ASHRAE* 13 (2007) 731–748.
- [15] M.O. McLinden, S.A. Klein, E.W. Lemmon, REFPROP – thermodynamic and transport properties of refrigerants and refrigerant mixtures, NIST Standard Reference Database, version 7, 2002.
- [16] H. Ju, Z. Huang, B. Buan, Y. Yu, Hydraulic performance of flow in small bending radius helical coil-pipe, *Journal of Nuclear Sci. and Tech.* 38 (10) (2001) 826–831.
- [17] Z.H. Chen, R.Y. Li, S. Lin, Z.Y. Chen, A correlation for metastable flow of R-12 through capillary tubes, *ASHRAE Trans.* 96 (1) (1990) 550–554.
- [18] A.E. Dukler, M. Wicks, R.G. Cleveland, Frictional pressure drop in two-phase flow. Parts A and B, *AIChE Journal* 10 (1) (1964) 38–51.
- [19] T.N. Wong, K.T. Ooi, Refrigerant flow in capillary tube: An assessment of the two-phase viscosity correlations on model prediction, *Int. Comm. Heat Mass Transfer* 22 (4) (1995) 595–604.